Physics of the Solid State, 2022, Vol. 64, No. 10

02,13

Fabrication of High-Quality Josephson Junctions Based on Nb|Al-AlN|NbN

© A.M. Chekushkin, L.V. Filippenko, M.Yu. Fominskiy, V.P. Koshelets

Kotelnikov Institute of Radio Engineering and Electronics, Russian Academy of Sciences, Moscow, Russia

E-mail: chekushkin@hitech.cplire.ru

Received April 29, 2022
Revised April 29, 2022
Accepted May 12, 2022

A description of the fabrication technology of high-quality tunnel SIS junctions is presented, with following characteristics: energy gap in superconductors $V_g = 3.2-3.4$ mV, tunnel current density up to J 35 kA/cm^2, quality factor R_j/R_n (ratio of subgap resistance to normal-state resistance) up to 30, junction area up to 1 μm^2. The SIS junctions are integrated into the NbTiN|SiO$_2$|Al microstrip line.

Keywords: superconducting devices, superconductor–insulator–superconductor tunnel junction, plasma etching.

DOI: 10.21883/PSS.2022.10.54222.49HH

1. Introduction

Modern problems of radio astronomy place high demands on the quality and parameters of the used SIS receivers. For receivers with operating frequencies up to 1 THz, for example [1,2], the key parameters are the high transparency of the tunnel barrier (currents 35 kA/cm^2 and higher), submicron tunnel junction area (1 μm^2 and below), as well as small leakage currents at resistances below the gap voltage. Nb-based Josephson junctions with aluminum oxide tunnel barrier (Nb|Al-AlO$_x$|Nb) do not allow to implement the required parameters [3,4], therefore, to solve the tasks, it was proposed to use tunneling Josephson junctions based on Nb|Al-AlN|NbN [5]. Selection for barrier of aluminum nitride is due to the fact that the aluminum oxide barrier (AlO$_x$) at values of the product of the junction area S and its resistance in the normal state R_n $R_nS \approx 20\,\Omega \cdot \mu$m^2 and less degrades, which leads to deterioration of volt-ampere characteristics (VACs). In addition, an important advantage of the aluminum nitride barrier is the ability to use NbN as the upper electrode of the tunnel structure. This, in turn, makes it possible to increase the gap voltage from 2.8 mV for structures made of niobium electrodes to 3.7 mV for Nb and NbN electrodes.

2. Fabrication

There are a number of methods for fabrication of Josephson junctions. The most developed, reliable, and well reproducible technology is the fabrication of SIS junctions based on niobium and its compounds using planar multilayer structures. Depending on the tasks, either high-resistance silicon ($> 10000\,\Omega \cdot$ cm) or amorphous quartz is chosen as the substrate for the samples. The process for fabrication of samples based on SIS junctions can be divided into the following main stages (Fig. 1): formation of a base electrode layer, formation of a SIS junction layer, anodization and deposition of insulation, formation of low electrode layer and a layer of gold contacts. As the manufacturing technology becomes more complex, additional steps may also occur, for example, the insulation layer, additional metallization layers, if it is necessary to form various transmission lines (microstrip one, coplanar one, or their combination). An Al$_2$O$_3$ layer 100 nm thick is deposited on the selected substrate by magnetron sputtering. This layer is necessary to avoid etching of the substrate material during subsequent technological operations. In this work, we used two methods for the formation of SIS junctions for the Nb|Al-AlN|NbN structure: through etching the upper NbN layer and through etching the three-layer structure. The latter is necessary for creating receiving structures with operating frequency up to 1 THz, which significantly exceeds „the gap“ frequency of niobium (700 GHz); NbTiN superconductor film with a larger energy gap was used as the lower electrode of the receiving element, and an Al film was used as the upper electrode.

Important criterion in the development of a technological map for the fabrication of samples is the minimum reproducible element of the microelectronic structure. Chemical liquid etching methods in this regard have significant limitations associated with isotropic etching and do not allow repeatable obtaining elements of submicron sizes. Dry etching method overcomes this problem. In addition, it has a number of advantages compared to wet chemical etching: the dry chemical etching process can significantly improve the accuracy of preparation samples of the required size, eliminate a large amount of toxic substances from production, reduce the degree of lateral undercut, and reduce the amount of by-products of etching compared to liquid chemical etching.

To fabricate samples with one etching, a bottom electrode pattern is formed on the substrate using a masking photore-

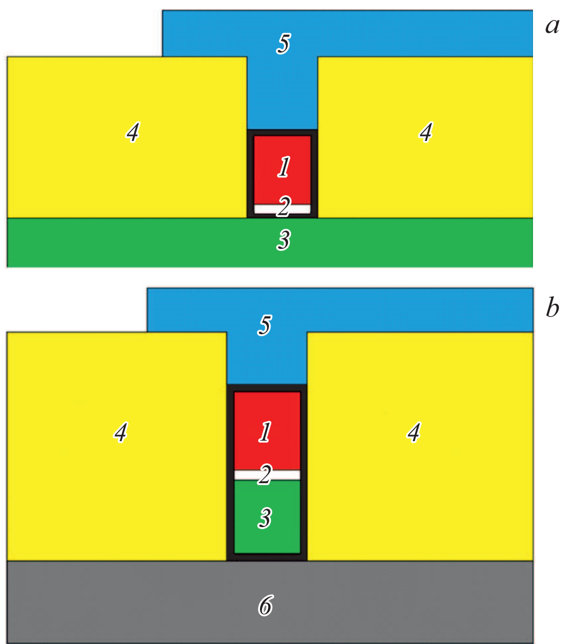

Figure 1. Lateral section of the SIS junction. *a*) Scheme of SIS junction formation using one etching: *1* — NbN (thickness 80 nm) (etched layer); *2* — Al-AlN (thickness 7−1 nm, respectively), *3* — Nb (thickness 200 nm), this layer plays the role of base electrode; *4* — SiO_2 insulator layer 250 nm thick; *5* — upper electrode made of aluminum (thickness 300 nm). *b*) Scheme of SIS junction formation by through etching of a three-layer structure: *1* — NbN (thickness 80 nm); *2* — Al-AlN (thickness 7−1 nm, respectively); *3* — Nb (thickness 80 nm); *6* — NbTiN (thickness 325 nm), which acts as a base electrode; *4* — SiO_2 insulator layer (thickness 350 nm); *5* — upper electrode made of aluminum (thickness 450 nm).

sist. Then, in a single vacuum cycle, the Nb|Al-AlN|NbN SIS structure is deposited with characteristic layer thicknesses of 200|7(1)|80 nm. Then, in dimethylformamide, heated to 60°C, the photoresist with the metal layer deposited on it is removed by explosive lithography (lift-off). After that, using a photolithography, a layer is formed that determines the geometry of the SIS junctions. Further, in the plant of plasma-chemical etching in a CF_4 gas atmosphere, the upper NbN layer is etched, the Nb surface and the side face of the SIS junctions are anodized, the SiO_2 insulation layer is sputtered, after which the lift-off occurs. The final stage of fabrication is the deposition of the upper electrode of aluminum.

Experiments were carried out to study the accuracy and uniformity of etching of micron-sized SIS junctions. Samples were etched in CF_4 atmosphere, under pressure $8 \cdot 10^{-2}$ mbar. Etching uniformity was studied over an area of $15 \times 15\,\text{mm}^2$, and the dimensions were controlled using a scanning electron microscope. SIS junctions of the same diameter were prepared on this area: 1.5 μm. The obtained sizes of SIS junctions during single-layer Nb etching were: minimum 1.46 μm (Fig. 2), maximum 1.54 μm (Fig. 3). The difference was 80 nm, and the deviation from the specified size was 40 nm. It is noteworthy that the samples located in close proximity to each other have the same dimensions (Fig. 3). In addition, a gradient of change in the linear size of the junction was observed: the largest one was below and left of the substrate, while the smallest one was up and right.

As part of the study of the effect of the presence of oxygen during plasma-chemical etching, the following experiment was carried out: a three-layer structure Nb|Al-AlN|NbN (80|7|80 nm) was prepared, then a resistive mask based on resist for e-beam lithography ma-N2403 was prepared, then, for better accuracy, windows were formed for SIS junctions by electron lithography, the same doses of light were used. Window diameter is 1 μm. Using a scanning electron microscope, the following parameters were controlled: the diameter of the window in the resist after the development of the resist, the diameter of the resist, and the diameter of the window after the etching procedure. Etching was carried out in two modes:

1. CF_4, power 50 W, pressure $8 \cdot 10^{-2}$ mbar.
2. $CF_4 + 3\%\,O_2$, power 50 W, pressure $8 \cdot 10^{-2}$ mbar.

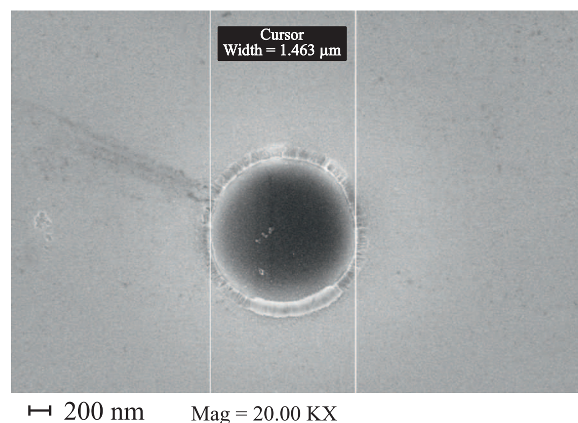

Figure 2. SEM photo of SIS junction and measured junction diameter.

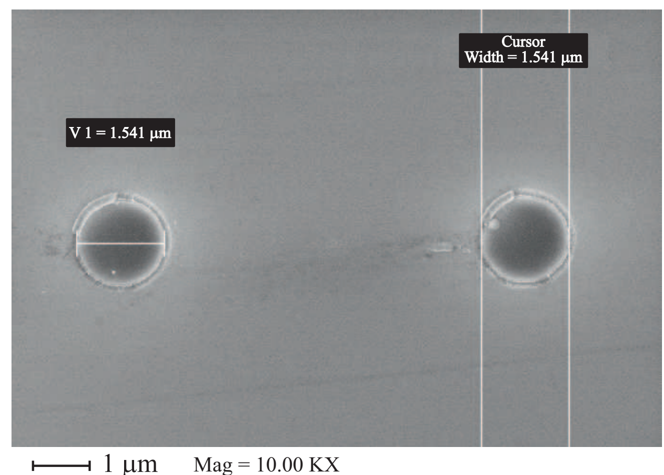

Figure 3. SEM photo of SIS junctions. Measured junction diameters.

In our experiment, not only the etching rate, but also the etching profile, both for the resist and for the metal, were controlled. This was made possible by scanning with electron microscope at an angle.

The difference in diameter at the base of the resist between the development of different samples was 10 nm: 990 nm versus 1000 nm. Both samples had a trapezoidal shape in cross section, with upper base of 887 and 891 nm, respectively. Example of a SEM photo for one of the samples is shown in Fig. 4.

After the niobium nitride was etched, the junction diameter was measured, the results of which are shown in Fig. 5, *a* and *b*. It can be seen that there are significant differences associated with the presence or absence of oxygen in the reactive gas mixture during plasma-chemical etching. This manifests itself in the fact that the presence of oxygen reduces the etching anisotropy and increases the lateral undercut, which led to a decrease in the lateral size by almost 150 nm. The absence of oxygen in the gas mixture makes it possible to achieve a more anisotropic etching, thereby preserving the vertical walls of the SIS junction and achieving more controlled and reproducible sizing of the SIS junctions, since etching without oxygen leads to decrease in the lateral size compared to the mask size by 7 nm.

For the case of formation of SIS junctions by through etching of Nb|Al-AlN|NbN, it is necessary to form on the substrate a base electrode. It is fabricated from the NbTiN layer, which is one of the electrodes for the NbTiN|SiO_2|Al microstrip transmission line. 325 nm NbTiN is deposited over the entire area of the substrate by DC magnetron sputtering. Then, according to the photoresist mask, according to the geometry of the base electrode, plasma-chemical etching of NbTiN is performed in a mixture of gases $CF_4 + 3\%\,O_2$: working pressure is $8 \cdot 10^{-2}$ mbar, power supplied to the electrode is 50 W. The preference for the formation of the base electrode by the plasma-chemical etching over the explosive lithography is due to the fact that the former makes it possible to achieve vertical walls of the material, which is important for the microwave properties of the microstrip line.

After the base electrode layer is formed, the Nb|Al-AlN|NbN SIS structure is deposited over the entire area of the substrate in one vacuum cycle. First, a Nb layer with a thickness of 80 nm is deposited onto the substrate by DC magnetron sputtering, then a thin Al layer with a thickness of 7 nm is deposited in the same way at a rate of 0.2 nm/s. After that, the AlN barrier is formed due to the nitridation of the Al layer in the nitrogen plasma discharge. It is important to note that the plasma discharge is initiated by applying voltage to the aluminum target, and not to the table on which the substrate is located. This approach makes it possible to achieve nitridation of the Al surface without damage to the film itself. The case of plasma initiation by applying a voltage to the table on which the substrate is located led to ion bombardment of the surface, which entailed a deterioration in the parameters of the AlN barrier. By varying the discharge power, as well as the process time,

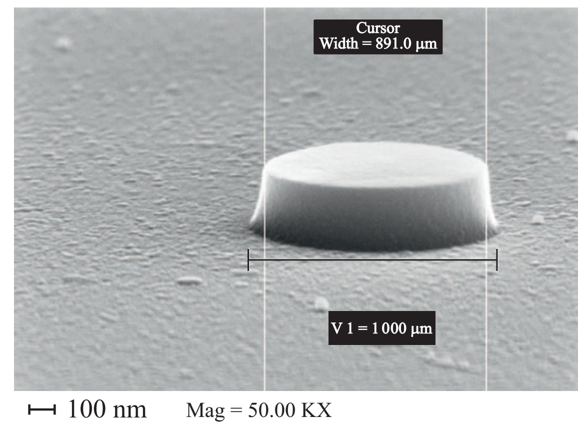

Figure 4. SEM photo at an angle: mask from photoresist with given diameter 1 μm.

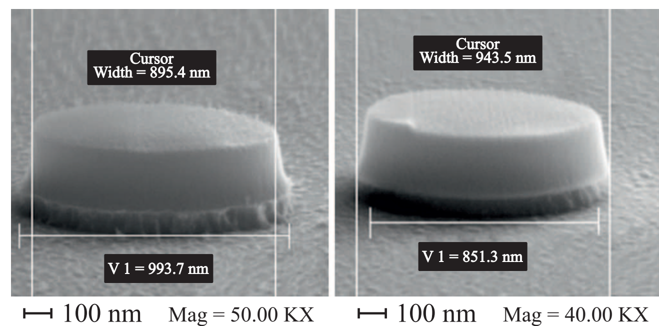

Figure 5. *a*) SEM photo after NbN etching in CF_4 atmosphere: mask from photoresist and NbN. *b*) SEM photo after NbN etching in $CF_4 + 3\%\,O_2$ atmosphere.

it is possible to achieve different barrier thicknesses, and as a result, different tunneling current through it, in the range from 200 A/cm^2 to 35 kA/ cm^2. The final stage is the deposition of NbN 80 nm thick. Its sputtering is performed with the help of DC magnetron with Nb target in the atmosphere of Ar:N_2 10:1 gas mixture. The film production modes and their calibration are described in more detail in the work [6,7].

The layer that defines the geometry of SIS junctions is formed using a photoresist mask. The characteristic junction diameter is $0.8-1.1\,\mu$m. Also on the manufactured samples present junctions of larger diameter (from 2 to 4 μm), necessary for test measurements and calculation R_nS. Initially, this is plasma-chemical etching of the upper NbN layer in CF_4 gas atmosphere. In contrast to the formation of the lower electrode (NbTiN), where a part of oxygen is used during etching, it was decided to use pure gas CF_4 when forming the SIS junctions. This approach made it possible to reduce the etching rate, which increases reproducibility (characteristic etching time is 1 min), as well as to reduce the loss of the resist, which was significantly higher in the case of the presence of oxygen during etching. The second step in etching is ion etching in the Ar atmosphere

in magnetron sputtering plant in the mode of setting the voltage on the sample holder: pressure $6 \cdot 10^{-3}$ mbar, power density $3.5\,W/cm^2$. The final plasma-chemical etching of the Nb layer is also carried out in an atmosphere of CF_4 gas: pressure $8 \cdot 10^{-2}$ mbar, power supplied to the electrode 50 W. After that, the same mask is used to anodize the NbTiN surface and the side walls of the SIS junctions in an ethylene glycol solution of ammonium pentaborate at voltage of 8−9 V. Then, the SiO_2 insulation layer is sputtered with a thickness of 250 nm. The lift-off is performed in a dimethylformamide solution in an ultrasonic bath, after which the formed SIS junctions are monitored by optical microscope.

In view of the fact that the NbTiN thickness is determined by the penetration depth of the magnetic field, and the insulation thickness — by the requirement for the characteristics of the microstrip line, it is necessary to locally make an additional insulation layer, which is SiO_2 with a thickness of 100 nm, to ensure full insulation coverage of the NbTiN thickness. The final stage of manufacturing is the formation of a contactor: the upper electrode of the microstrip line made of Al 450 nm thick.

When forming SIS junctions, reactive ion etching is used, which significantly increases the surface roughness. After the removal of the Al-AlN layer in this process, the root-mean-square deviation of the Nb surface profile can reach 11.6 nm [8]. This can adversely affect the performance of the microstrip transmission line, since the subsequent plasma-chemical etching is not selective between Nb and NbTiN, which leads to undercutting of the NbTiN layer, while the Nb layer acts as a mask. To avoid deterioration of the NbTiN surface roughness, it was decided to deposit a thin layer (5 nm) of aluminum in the cycle of forming a three-layer SIS structure, which works as a stop-layer for plasma-chemical etching in fluorine-containing gases. Subsequent measurements have shown that this layer has no noticeable effect on the volt-ampere characteristics of the junctions, but it makes it possible to avoid NbTiN etching.

3. Measurements

The IV-curve of the SIS junction makes it possible to obtain the following characteristics: the value of the energy gap in the superconductor V_g, the spreading of the gap ΔV_g, the tunneling current density J, and the quality parameter, which is defined as the ratio of subgap resistance R_j to the resistance in the normal state R_n and characterizes the subgap leakage current. The measurements were performed by immersing the cryogenic insert in the Dewar vessel filled with helium at a temperature of 4.2 K. The DAC−ADC switching board and the IRTECON data acquisition system [9] were used for the measurement. The IV-curves of the prepared SIS junctions were measured: by the method of single etching of NbN (Fig. 6) and by the method of through etching of the Nb|Al-AlN|NbN structure (Fig. 7). Comparison of the two technologies (etching of

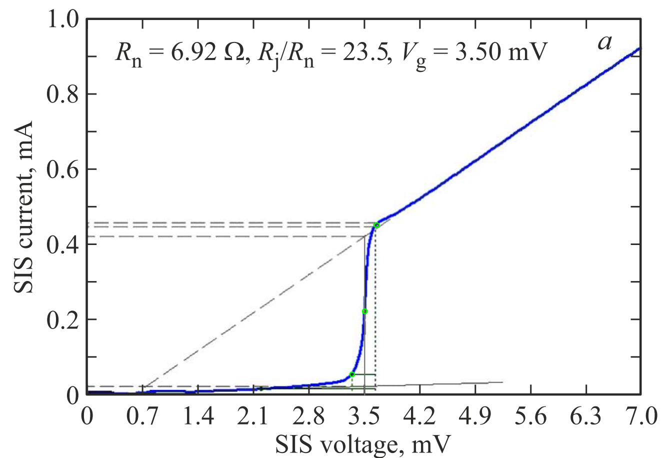

Figure 6. IV-curve of the Nb|Al-AlN|NbN junction with one etching, $R_nS = 8\,\Omega \cdot \mu m^2$.

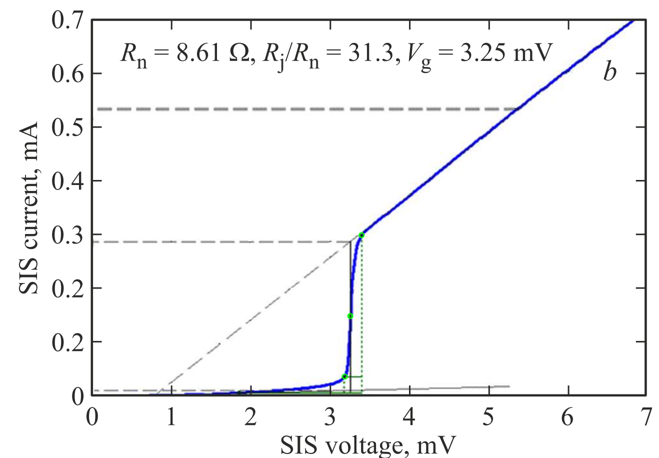

Figure 7. IV-curve of the Nb|Al-AlN|NbN junction with through etching, $R_nS = 8\,\Omega \cdot \mu m^2$.

one layer or etching of three layers in the SIS junction) showed that the location of the SIS junction on the NbTiN electrode leads to decrease in the energy gap from 3.5 to 3.25 V. The developed approaches and technologies will be in demand in the manufacture of receiving elements of low-noise THz-range receiving systems for new ground-based and space radio astronomy projects [10,11].

4. Conclusion

Tunnel junctions Nb|Al-AlN|NbN are fabricated by the through etching of the structure. Measurements of their IV-curves showed that this method is suitable for creating SIS structures with a high current density and a junction area of the order of $1\,\mu m^2$ and will be used to create ultrasensitive receivers for new radio astronomy projects.

Funding

This study was supported financially by the RFBR (project No. 19-52-80023 BRICS_t). Tunnel junctions were fabricated under the state assignment of the Kotelnikov Institute of Radio Engineering and Electronics of RAS. For the manufacture of samples, the equipment of Unique Scientific Facility #352529 „Cryointegral“ was used, the development of which was supported by a grant from the Ministry of Science and Higher Education of the Russian Federation, agreement No. 075-15-2021-667.

Conflict of interest

The authors declare that they have no conflict of interest.

References

[1] A.V. Khudchenko, A.M. Baryshev, K.I. Rudakov, P.M. Dmitriev, R. Hesper, L. de Jong, V.P. Koshelets. IEEE Trans. Terahertz Sci. Technol. **6**, *1*, 127 (2015).
[2] K.I. Rudakov, A.V. Khudchenko, L.V. Filippenko, M.E. Paramonov, R. Hesper, D.A.R. da Costa Lima, A.M. Baryshev, V.P. Koshelets. Appl. Sci. **11**, *21*, 10087 (2021). DOI: 10.3390/app112110087
[3] A.W. Kleinsasser, R.E. Miller, W.H. Mallison, G.B. Arnold. Phys. Rev. Lett. **72**, *11*, 1738 (1994).
[4] B. Bumble, H.G. LeDuc, J. Stern. Proc. 9th Int. Symp. Space THz Technol., CIT, PC. 295 (1998).
[5] M.Yu. Torgashin, V.P. Koshelets, P.N. Dmitriev, A.B. Ermakov, L.V. Filippenko, P.A. Yagoubov. IEEE Trans. Appl. Supercond. **17**, *2*, 379 (2007).
[6] A.M. Chekushkin, L.V. Filippenko, A.A. Lomov, D. Liu, S.-C. Shi, V.P. Koshelets. ZhTF **91**, *10*, 1577 (2021) (in Russian).
[7] M.Y. Fominsky, L.V. Filippenko, A.M. Chekushkin, P.N. Dmitriev, V.P. Koshelets. Electronics 2021, **10**, *23*, 2944 (2021). https://doi.org/10.3390/electronics10232944
[8] A.M. Chekushkin, L.V. Filippenko, V.V. Kashin, M.Y. Fominskiy, V.P. Koshelets. RENSIT **13**, *4*, 419 (2021).
[9] A.B. Ermakov, S.V. Shitov, A.M. Baryshev, V.P. Koshelets, W. Luinge. IEEE Trans. Appl. Supercond. **11**, *1*, 840 (2001).
[10] https://www.eso.org/public/teles-instr/apex/ (accessed on 14 April, 2022).
[11] http://millimetron.ru/index.php/en/ (accessed on 14 April, 2022).